# CFD MODELLING OF LED HEAT SINK: GEOMETRIC OPTIMIZATION

YEOW YEE SIN

UNIVERSITI TEKNIKAL MALAYSIA MELAKA

# CFD MODELLING OF LED HEAT SINK: GEOMETRIC OPTIMIZATION

**YEOW YEE SIN**

**A report submitted**
**in fulfillment of the requirements for the degree of**
**Bachelor of Mechanical Engineering**

**Faculty of Mechanical Engineering**

**UNIVERSITI TEKNIKAL MALAYSIA MELAKA**

**2020**

## DECLARATION

I hereby declare this project report entitled "CFD Modelling of LED Heat Sink: Geometric Optimization" is the result of my own research except as cited in the references.

Signature : …………………………

Name : …………………………

Date : …………………………

## APPROVAL

I hereby declare that I have read this project report and in my opinion this report is sufficient in terms of scope and quality for the award of the degree of Bachelor of Mechanical Engineering.

Signature : ...........................

Supervisor's Name : ...........................

Date : ...........................

# ABSTRACT

Natural convection heat transfers around a horizontal rectangular heat sink still provide too much of significance in dissipating the waste heat generated by Light Emitting Diode (LED) into the air. The present study aims to propose an efficient heat sink without increasing production cost to obtain better heat transfer rate by natural heat transfer convection without excessive usage of material. An approach that is changing the fin mass distribution across the heat sink under the constraint of a fixed total mass of fin materials has been studied. The numerical results were compared with experimental results and it showed a good agreement. To select the optimal configuration of fins, three different types of heat sink (Flat, Convex, and Concave models) were compared. The flow field pattern around the fins was observed and it can be concluded that decreasing the fin height from the outer side to the inner side of the heat sink can produce a high rate of heat transfer. By comparing the average heat transfer coefficient of the three models, the Concave model is selected as the optimal configuration of fins. This is because the Concave model has more than 20% improvement in the average heat transfer coefficient as compared to the Flat model. Whilst, Convex model has more than 20% reduction in average heat transfer coefficient as compared to the Flat model. Finally, the optimization for the average heat transfer coefficient considering various fin height and heat sink base thickness was performed. It was able to produce a maximum average heat transfer coefficient of 10.4136 $W/m^2K$ at optimal settings of fin height and heat sink base thickness.

## ABSTRAK

*Pemindahan haba perolakan semula jadi di sekeliling sinki haba yang bersegi empat tepat mendatar masih memberikan impak yang besar dalam pelepasan sisa haba yang dihasilkan oleh Pencahayaan Diod Pemancar Cahaya (LED) ke udara. Tujuan penyelidikan ini adalah untuk mencadangkan sinki haba yang cekap tanpa meningkatkan kos pengeluaran supaya mendapatkan kadar pemindahan haba yang lebih baik dengan perolakan pemindahan haba semula jadi tanpa menggunakan bahan berlebihan. Pendekatan yang mengubah pengedaran jisim sirip sepanjang sinki haba di bawah kekangan jumlah jisim bahan sirip yang tetap telah dikaji. Keputusan simulasi dibandingkan dengan keputusan eksperimen dan ia menunjukkan persetujuan yang baik. Untuk memilih konfigurasi sirip yang optimum, tiga jenis sinki haba (model Flat, Convex, dan Concave) telah dibandingkan. Corak medan aliran di sekitar sirip diperhatikan dan ia dapat disimpulkan bahawa penurunan ketinggian sirip dari kawasan luar ke kawasan dalam sinki haba (jenis Concave) dapat menghasilkan kadar pemindahan haba yang tinggi. Dengan membandingkan purata pekali pemindahan haba ketiga-tiga model tersebut, model Concave dipilih sebagai konfigurasi sirip yang optimum. Hal ini kerana model Concave mempunyai lebih dari pada 20% peningkatan dalam purata pekali pemindahan haba apabila membanding dengan model Flat. Manakala, model Convex pula mempunyai lebih daripada 20% pengurangan dalam purata pekali pemindahan haba apabila membanding dengan model Flat. Akhirnya, pengoptimuman purata pekali pemindahan haba dengan mempertimbangkan pelbagai ketinggian sirip dan ketebalan dasar sinki haba telah dijalankan. Ia dapat menghasilkan purata pekali pemindahan haba yang maksimum, iaitu 10.4136* $W/m^2K$ *dalam tetapan ketinggian sirip dan ketebalan dasar sinki haba yang optimum.*

## ACKNOWLEDGEMENTS

First of all, I wish to express my sincere thanks to my supervisor Dr. Cheng See Yuan from the Faculty of Mechanical Engineering, Universiti Teknikal Malaysia Melaka in guiding me throughout this research. I am extremely grateful to him for sharing his expertise and encouragement during the entire period of this project.

Besides, I would like to thank my parents Mr. Yeow Hoo Jee and Mrs. Goh Bee Yong for always giving support, encouragement, and attention to me.

Last but not least, I would like to express my thankful to my coursemate Fong Yee Pin and Lim Heng Yang for guiding me during the final year project. I am grateful that I had met a bunch of friends who always helping me throughout my life as a student at university.

# TABLE OF CONTENT

## LIST OF FIGURES

# LIST OF TABLES

## LIST OF SYMBOLS

| | | |
|---|---|---|
| S | = | Fin spacing |
| H | = | Fin height |
| th | = | fin thickness |
| 2L | = | total length of the fin |
| t | = | thickness of fin arrays |
| L | = | Length of fin |
| n | = | Number of spacing in fin arrays |
| $t_b$ | = | Heat sink base thickness |
| $\lambda$ | = | Thermal conductivity |
| $\alpha$ | = | Thermal expansion |
| h | = | Convective heat transfer coefficient |
| $\rho_e$ | = | Electrical resistivity |
| E | = | Modulus of elasticity |
| $\rho$ | = | Density |
| C | = | Cost |
| Q | = | Total heat transfer rate from fin arrays to the surrounding |
| A | = | Total heat transfer area of the fin arrays |
| $\Delta T$ | = | Temperature difference between the base surface and ambient air, $(T_b - T_a)$ |
| $T_b$ | = | Base surface temperature |
| $T_a$ | = | Ambient temperature |
| u | = | x-component of velocity (m/s) |
| v | = | y-component of velocity (m/s) |

| | | |
|---|---|---|
| w | = | z-component of velocity (m/s) |
| g | = | gravity, $m/s^2$ |
| μ | = | dynamic viscosity, N/$m^2$s |
| $c_p$ | = | coefficient of heat capacity, J/(kg°C) |
| $\beta$ | = | coefficient of thermal expansion |
| $Gr_H$ | = | Grashof number with respect to fin height |

# CHAPTER 1

# INTRODUCTION

## 1.1 BACKGROUND

A light-emitting diode is a semiconductor device that emits light when current flow through it. Light-Emitting Diode usually denoted by the term LED. LEDs are comprised of compound semiconductor materials, such as gallium phosphide (GaP), gallium arsenide phosphide (GaAsP), and gallium arsenide (GaAs). LED light emits energy in the form of light. Practically, it also discharges energy in the form of heat. A typical LED can produce about 70% of total energy consumed as heat and thus creating a thermal problem.

Waste heat dissipation from LED gives a major impact on the performance of LED. The temperature of LED will rise due to improper dissipating of heat by a cooling system. An inefficient heat sink can cause damage to the LED's component as the temperature increases (Li et al., 2010). Besides that, the presence of waste heat will also lead to lumen degradation. Therefore, a better design of a heat sink is needed to promote heat transfer and to dissipate the waste heat properly.

A suitable cooling solution that can simply move waste heat generated by LED into the air is called a heat sink. In other words, a heat sink can transfer the heat or thermal energy from high-temperature to a low-temperature medium like air by natural convection cooling or forced air cooling. The forced air convection is the most effective solution but it is costly due to it requires some space for the installation of blower and ductwork (Amit Shah et al., 2006). So, it is important to choose effective cooling solutions to preserve the reliability of the electronic device.

The optimization of heat sink geometry is one of the most essential solutions in enhancing the thermal performance of the heat sink. The fin shape, number of fins and orientation of the fins are some of the factors on improving the thermal performance of heat sink. Besides that, various fin mass distribution across a rectangular heatsink under a fixed mass of fin material also may overcome the problems that the heatsink could not dissipate waste heat properly, which is a low average heat transfer coefficient or low heat transfer rate. These solutions are considered a cost-effective method in improving the thermal performance of heatsink because there is no excessive usage of materials in which the mass of the heat sink is kept constant throughout the distribution of fin materials.

Many tools like CFD (Computational Fluid Dynamic) and Ansys are most commonly used for heat sink optimization. With a new optimal heat sink design, LED lighting might be able to dissipate the heat effectively.

## 1.2 PROBLEM STATEMENT



Although many effective types of heat sinks have been created to dissipate more heat in LED light, the thermal problem still exists. The main challenge is to propose an efficient heat sink with a better heat transfer rate by natural heat transfer convection. Many LEDs have to face a certain amount of waste heat because of the poor and ineffective heat sink. The shortcomings of heat sink had made LED's manufacturer investigate new potential heat sink that has a bigger surface area at transferring heat.

The flow of fresh air into the heat sink is strongly impacted by the mass distribution of fins on a heat sink. The larger mass distribution of the fin can reduce fluid flow resistance, in which allowing more cooling air to enter through a heat sink. A heat sink is designed by using high usage of materials that have more mass distribution and this property makes the heat sink more expensive. Thus, the optimization of fin mass distribution must be good enough to dissipate heat and be able to produce a heat sink without excessive usage of materials.

## 1.3 OBJECTIVE

The main objective of this research is as follow.

1. To determine the optimal configuration of fins under constraint of fixed total mass and fixed mass of fin material.
2. To study the effect of fin mass distribution across heatsink towards average heat transfer coefficient.

## 1.4 SCOPE OF THESIS



The scope of this thesis are:

1. Analysis study on heat removal by heat sink under natural convection.
2. Comparative study on the effect of different configuration of fin on dissipating heat to the environment.
3. Geometry optimization of LED heat sink by using rectangular heat sink.
4. Heat transfer through the rectangular base is keep constant.
5. Radiation heat loss at the heat sink is negligible.

## 1.5 GENERAL METHODOLOGY

In this research, an approach that needed to be employed to achieve the objectives are shown as following.

1. Literature review

   The journal, websites, book or any source related to the project will be studied.

2. Visualization

   Visualization by using Computer Fluid Dynamics (CFD) to get see fluid flow pattern in heat sink.

3. Evaluation

   The selection of optimum configuration of fin and how the configuration of fin affects the average heat transfer coefficient will be discussed.

4. Prepared summary report

   At the end of the research, a report of this research will be written.

# CHAPTER 2

# LITERATURE REVIEW

## 2.1 LED Heat Sink

Heat sink is a very important fixture in a light-emitting diode (LED) because it can remove an excessive waste of heat produce by LED as the temperature rise. The effectiveness of every component in electronic devices depends on temperature, in which higher temperatures will become harmful to the reliability of these devices (Shah et. al. 2006). Therefore, an efficient heat sink is needed to promote the heat transfer rate and prevent electronic devices from overheating. To select a good quality of heat sink, there are some factors needed to be considered which are material selection, shape of a fin, surface treatment and mass flow rate of fresh air.

### 2.1.1 Horizontal Rectangular Fin Arrays



The fin array configuration of the heat sink is shown in Figure 2.1. As observed, the heat sink is constructed by using a horizontal rectangular fin and horizontal base plate. The finned surface is widely used in a variety of engineering applications because it provides a greater heat transfer area for heat transfer.

First, the process of heat transfer is started by natural convection on a finned surface. Natural convection on a surface depends on the geometry and orientation of the surface. According to Harahap & McManus (1967), the single chimney flow pattern had better heat transfer performance as compared to a sliding chimney flow pattern. Besides that, model details of natural convection for vertical rectangular fins with constant length on the vertical base can be found from an experimental study of Welling and Woolbridge. Based on the experiment carried out by Welling & Woolbridge (1965), the fin height is greatly impacted by the fin spacing, in which there is an optimum fin height for each fin spacing.

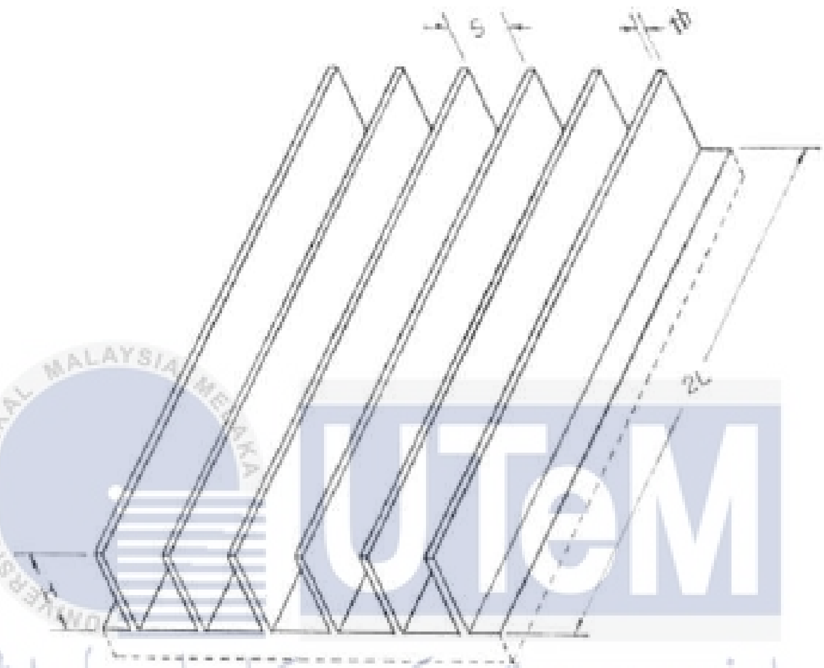

Figure 2.1: Fin array configuration (Harahap et. al, 1967)



### 2.1.2 Material of Heat Sink

For the selection of heat sink materials, thermal material with high thermal conductivity and low coefficient of thermal expansion are preferable (Ekere et. al. 2011). Based on the research studied by G. Prashant Reddy & Navneet Guptal (2010), a heat sink material with high thermal conductivity can increase the heat transfer rate. They suggested that aluminum-based alloys or metals are very optimistic materials for the heat sink. There were two case studies clearly stated by them as shown in Table 2.1.

Table 2.1: Material selection requirements (G. Prashant Reddy & Navneet Guptal, 2010).

| Cases | Case 1 | Case 2 |
|---|---|---|
| **Function** | Heat Sink | Heat Sink |
| **Constraints** | Material must have $p_e > 10^{19} \mu\Omega\ cm.$<br>All dimensions specified. | Temperature and volume of material decrease.<br>High electrical resistivity.<br>High value of Young's modulus, thermal expansion must be emphasize. |
| **Objectives** | To increase thermal conductivity | Maximize Young's modulus<br>Heat transfer coefficient increase, temperature increase |

The graph was simulated by software based on Case 1 condition as showed in Figure 2.2. As shown in Figure 2.2, Aluminum nitrate (AIN) or Alumina $Al_2O_3$ meet the requirement for the Case 1 condition.

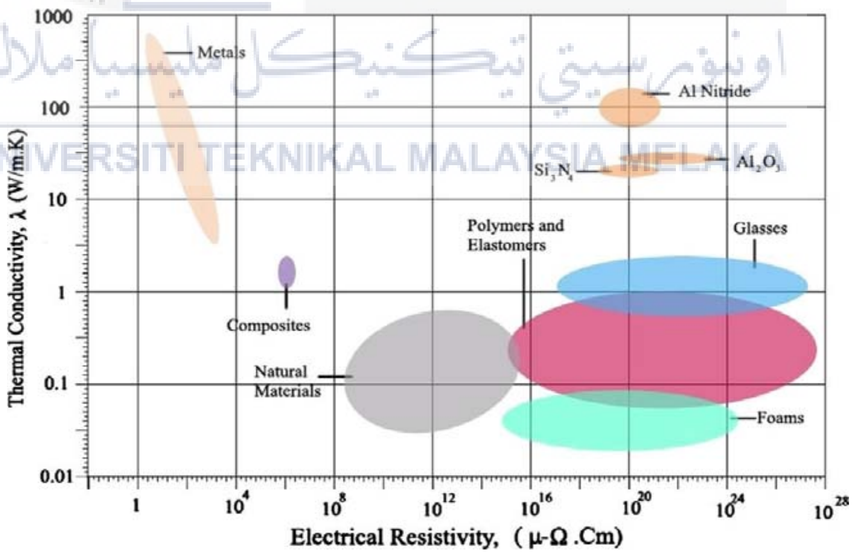


Figure 2.2: Effect of thermal conductivity toward electrical resistivity for different type of materials

(G. Prashant Reddy & Navneet Guptal, 2010)

The graph was simulated by software based on Case 2 condition as showed in Figure 2.3. As shown in Figure 2.3, Al, AIN, $Al_2O_3$ meets the requirement for the Case 2 condition.

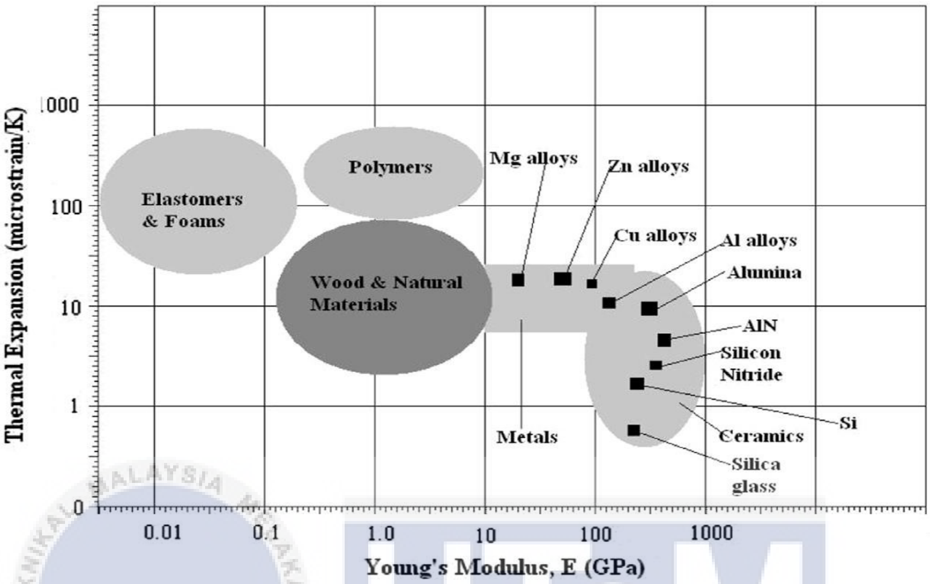


Figure 2.3: Effect of thermal expansion toward young's modulus for different type of materials (G. Prashant Reddy & Navneet Guptal, 2010)

Based on the above approach, the aluminum-based alloy is the best material to design a heat sink for the use of heat removal in microelectronic.

Furthermore, aluminum is the best choice material for producing heat sink devices (Almomani et. al. 2018). They have shown that the selection of material is based on six criteria which are thermal conductivity, thermal expansion coefficient, electrical resistance, modulus of elasticity, cost, and density. They applied a decision making technique called the Analytical Hierarchy Process (AHP) to select the best choice materials for heatsink devices.

Table 2.2: Selection criteria for heat sink material and required direction of change for each criterion (Almomani et. al. 2018).

| **Selection criterion** | **Symbol** | **Required direction of change** |
|---|---|---|
| Thermal conductivity | $\lambda$ | Maximize |
| Thermal expansion | $\alpha$ | Minimize |
| Convective heat transfer coefficient | h | Maximize |
| Electrical resistivity | $\rho_e$ | Maximize |
| Modulus of elasticity | E | Maximize |
| Density | $\rho$ | Minimize |
| Cost | C | Minimize |

Table 2.3: List of the values of the selection properties (Online Material Information Resource, 2018)

| Property | $\lambda$ | $\alpha$ | $\rho_e$ | E | $\rho$ | C |
|---|---|---|---|---|---|---|
| Material | W/m.K | $10^{-6}$/°C | $\Omega.cm$ | GPa | g/$cm^3$ | |
| S-65C | 216 | 14.5 | 4.3 x $10^{-6}$ | 303 | 1.844 | Extreme high |
| AIN | 140-180 | 4.5 | >$10^{14}$(5x$10^{14}$) | 330 | 3.26 | High |
| Al | 237 | 23.1 | 2.82x$10^{-6}$ | 70 | 2.7 | Very low |
| Cu | 401 | 16.5 | 1.678x$10^{-6}$ | 110-128 | 8.96 | Medium |
| Al5050-O | 193 | 24.7 | 3.49x$10^{-6}$ | 68.9 | 2.69 | Low |



Based on the requirement showed in Table 2.3, aluminum is the perfect choice for the heatsink devices due to its good thermal conductivity with low density and acceptable cost.

## 2.2 Natural Convection

In recent years, electronic devices are targeting in smaller sizes with high capacity, high efficiency, and producing more heat. Typically, the working temperature of electronic devices ranges from 85 to 100℃. The electronic device's component performance decrease by 5% and the lifespan reduces dramatically when the temperature rises every 1℃ above the limit temperature (Ahmed et. al. 2017). Therefore, the high heat generated is detrimental to the reliability and usable life of the electronic components. Thus, a suitable cooling method to remove the high heat produced by electronic components needs to be investigated and developed. There are various cooling techniques for heat dissipating through heat sinks categorized as following (Khattak et. al. 2016).

(1) Passive techniques
   - Cooling via natural convection by changing the geometrical flow channels of the heat sinks.

(2) Active techniques
   - These use external power input such as moving fans for heat transfer enhancements.

(3) Compound techniques
   - Mixing of active and passive techniques in improving the heat transfer performance. This technique is used in complex design.

For the study of active cooling systems, forced air convection is the most suitable solution for high-end applications. In this case, the high velocity of air is forced through the heat sink and thus undergo rapid convective heat transfer. Nevertheless, this approach is costly because of the high velocity in the system will increase the noise level and pressure drop will occur due to frictional effect (Shah et. al. 2006). In other words, inserting a blower to the system can lead to an increase in the surface area and thus increasing the overall weight and cost.

As in the passive cooling technique, natural convection is used for consumer LED lighting with the application of heat sink. According to Ostrach (1988), the natural convection is most commonly used to remove the waste heat due to its simplicity, less cost, low noise, small in size, and reliability. There were some advantages of natural convection from heat sink showed by J.R. Pryde & D.C. Whalley, (2014) at $14^{th}$ IEEE Intersociety Conference on Thermal and Thermomechanical Phenomena in Electronic Systems.

Advantages of Natural Convection from Heat Sink

- ✓ Long usable lifespan
- ✓ Highly cost effective
- ✓ Zero power consumption
- ✓ Low to zero maintenance
- ✓ Less noise

In natural convection, the natural convection current is caused by the two forces, which are buoyant force and friction force. According to S. Mostafa Ghiaasiaan (2011), the motion of fluid due to the forces of the body and its dependence on the fluid density are sensitive to the temperature of the fluid. The formula that describes the average heat transfer coefficient in the cooling system under natural convection is defined as following (Dialamah et. al. 2008).

$$h = Q/A\Delta T$$

where Q = Total heat transfer rate from fin arrays to the surrounding

A = Total heat transfer area of the fin arrays

$\Delta T$ = $T_b$ - $T_a$

= Temperature difference between the base surface and ambient air

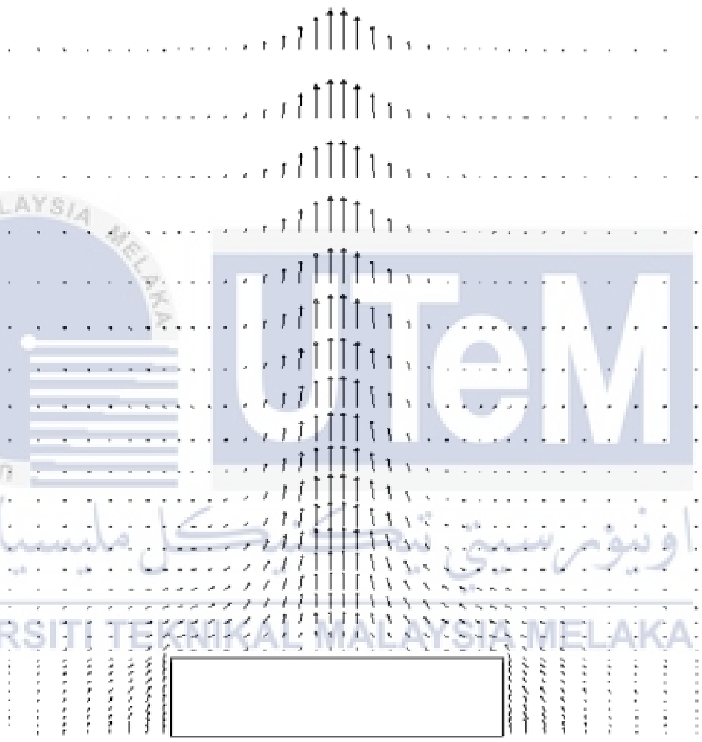



Figure 2.4: Flow pattern of natural convection in horizontal rectangular fins

(Dialameh et al, 2008)

There were several experimental investigations on the optimization of a heat sink in natural convection by the researcher. (Starner & McManus, 1963) conducted the experimental study on four different arrangements of fin arrays with different dimensions toward the heat transfer coefficient. They stated that the improper design of fin to a surface could decrease the total heat transfer rate. Besides that, (Harahap &

McManus, 1967) studied the effect of two different fins length towards the average heat transfer coefficient and also conducted observation on flow field patterns. From their observation, they found that single chimney flow patterns produce a better heat transfer rate than a sliding chimney flow pattern.

## 2.3 Geometric Optimization of Heat Sink

The effects of the different geometric parameters of a heat sink with an average heat transfer coefficient were carried out. There was a numerical study on horizontal rectangular thick fin arrays (3mm < t < 7mm) with a short length (L ≤ 50mm) under natural convection (Dialameh et. al. 2008). The researcher studied the Rayleigh and Nusselt number based on different fin geometries and temperature variation.

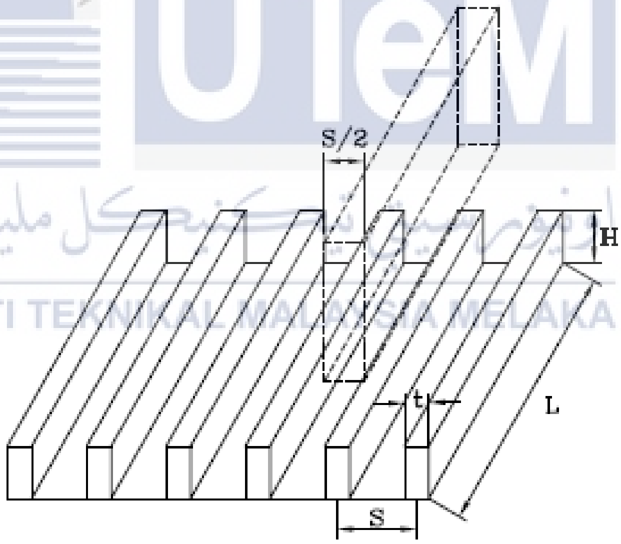


Figure 2.5: Fin arrays of Heat Sink (Dialameh et. al. 2008)

In this model, the flow field pattern of the heat sink was visualized, in which the second type of flow pattern exhibited a lower heat transfer coefficient than the first type of flow pattern. Besides that, this model also showed that the natural convection heat transfer coefficient increases with increasing temperature difference and fin spacing, but decreasing with fin length.

### 2.3.1 Flow Pattern of Heat Sink

In order to visualize the flow field pattern, the airflow velocity is plotted at several cross-sections in the channel. Figures 2.6 and 2.7 showed the first flow type and second flow type respectively. For the first flow type, air flows from the open boundaries, travel through the length of the fin and spreads out in the middle of the channel. For the second type flow, air can enter the middle of the channel, flows around the base surface, and finally travel along with the height of fins as it passed towards the middle part of the channel. These two observations were stated by Dialameh et al, (2008) after compared with the experimental study on horizontal rectangular fin arrays under natural convection heat transfer by Harahap & McManus, (1967).

There was a study of the optimum parameters of heat sink related to the velocity profile of different geometric parameters carried out by Dialameh et al, (2008). Velocity profiles proposed in this study able to prove that the combination of fin height, fin length and fin spacing can affect the flow field pattern and natural convection heat transfer around the heat sink. Besides that, the flow pattern also indicates that H/L and S/L parameters affect the amount of fresh air enter the channel and produce plume above the fins. The three velocity profiles that were plotted in this study showed in Figures 2.6 to 2.8.

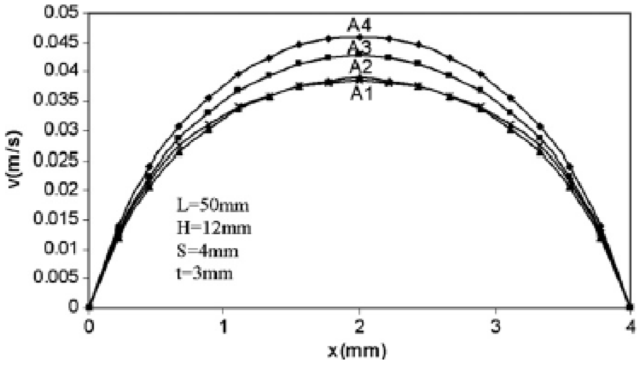


Figure 2.6: Velocity profiles of first flow type (Dialameh et. al. 2008).

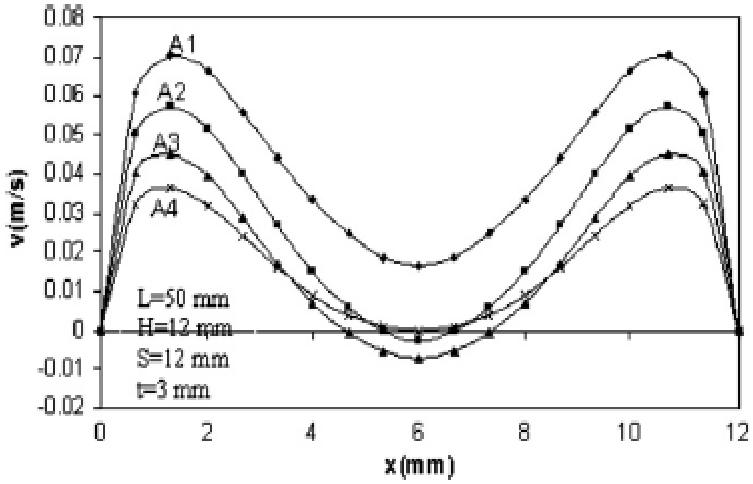


Figure 2.7: Velocity profiles of second flow type (Dialameh et. al. 2008).

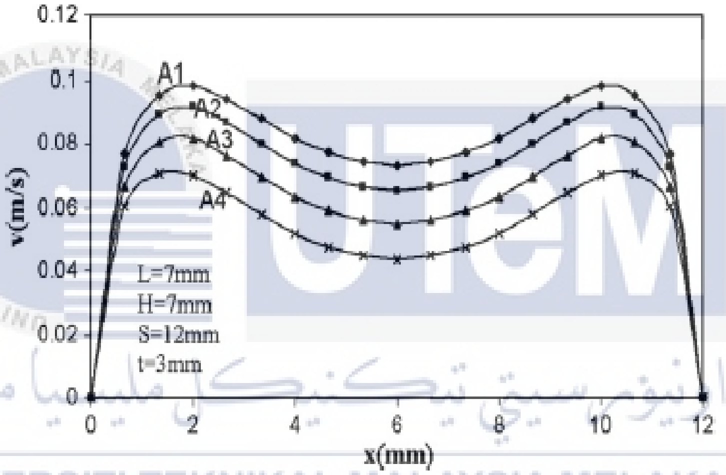




Figure 2.8: Velocity profiles of shortest fin arrays (Dialameh et. al. 2008).

### 2.3.2 Geometric Parameter of Fin Length

According to Dialameh et al, (2008), the numerical result for the effect of fin length with two different fin thicknesses as graphically shown in Figure 2.9. For these results, it is showed that the average heat transfer coefficient decreases significantly with increasing fin length. As shown in Figure 2.9, there was a small change in the average heat transfer coefficient when comparing two different thickness of fins. Thus, his study showed that a shorter length of the fin can enhance heat transfer performance and prevent the heat sink from overheating. Besides that, they also reported that fin thickness gives a small effect on the average heat transfer coefficient.

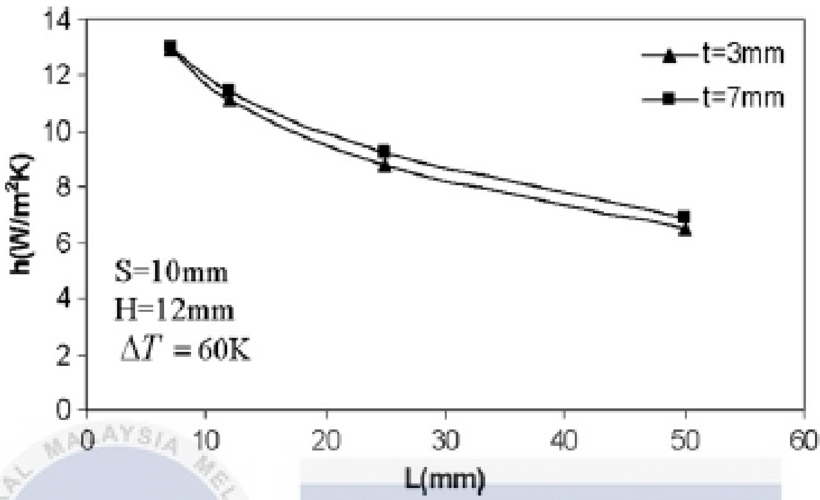


Figure 2.9: The effect of fin length with thickness of fin (Dialameh et. al. 2008).

### 2.3.3 Geometric Parameter of Fin Spacing



There was a combination studied of geometric parameters on average heat transfer coefficient conducted by Dialameh et. Al, (2008). The research implies that the relationship between such parameters can affect the average heat transfer coefficient. The study concluded that the average heat transfer coefficient increases with increasing the ratio of fin height to fin length, H/L and the temperature difference. Figure 2.10 showed the graphical result of the average heat transfer coefficient versus the fin spacing with two temperature differences and different H/L.

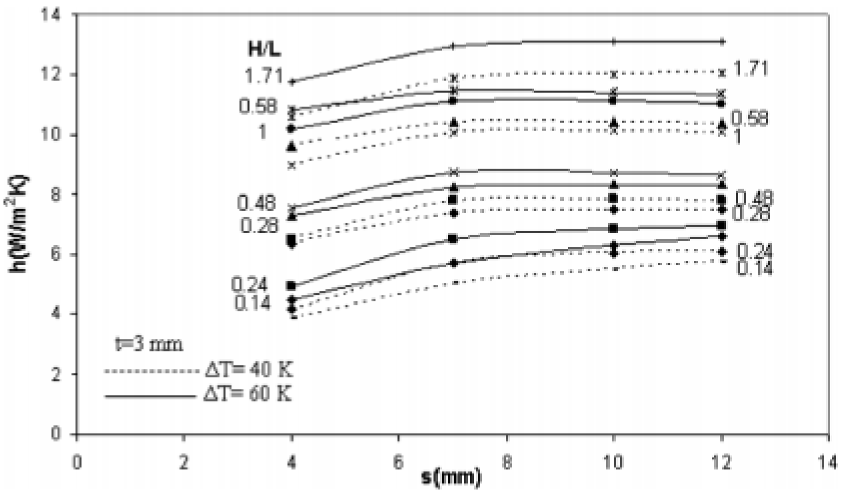


Figure 2.10: The graph of average heat transfer coefficient versus fin spacing with two temperature difference and different H/L (Dialameh et. al. 2008).

## 2.4 Numerical Simulation

For validation of the results, the numerical method was applied to simulate with the experimental results. In this case, there was a small difference between the numerical results and the experimental results. Thus, the research was able to simulate the results with experimental results because the difference is less than 3.0% (Dialameh et. al. 2008).

There was a comparative study on average heat transfer coefficient over temperature difference with the experimental results studied by Harahap & McManus, (1967). In Figure 2.5, the present study shown good compliance with experimental measurements.

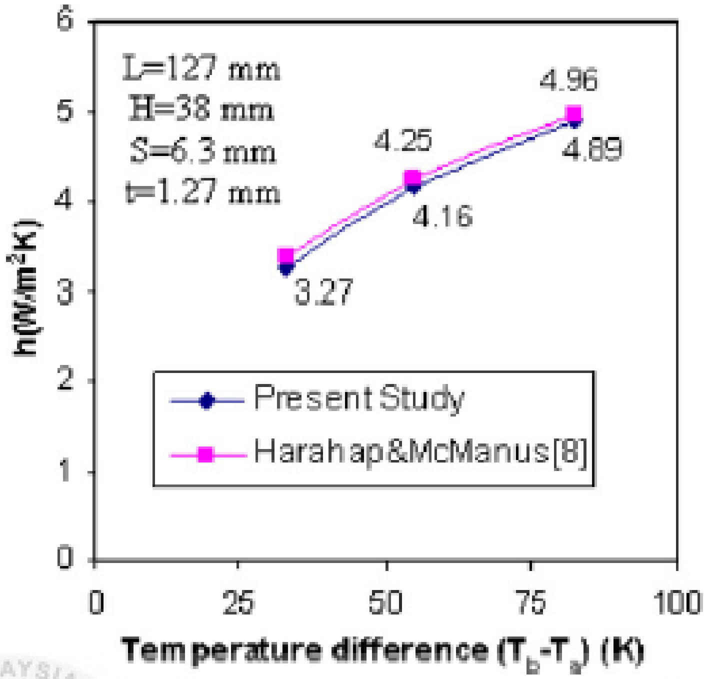


Figure 2.11: Numerical analysis of average heat transfer coefficient toward temperature differences (Dialameh et. al. 2018).

# CHAPTER 3

# METHODOLOGY

## 3.1 Introduction

In this chapter, the methodology employed in this research will be explained. As shown in Figure 3.1, the flowchart represented the process of the project and the flow of every component involved in this project. Firstly, the literature review will be studied to understand the effect of various parameters of the heat sink on the heat transfer performance. It helps to understand the fundamental of theory in this research.

To achieve the objective of the present study, Ansys Ver 16.0 software is used for heat sink optimization and simulation. The fin arrays and the computational domain are constructed by using Ansys Workbench. The fins are arranged by following the variation of sinusoidal shaped. A computational domain is created where the domain is minimized to one-quarter of the total fin array. The symmetry boundary condition is used on the repetitive characteristics of the heat sink geometry. Next, the grid is created on the geometry model.

For the boundary condition, the viscous laminar model is applied to all cases due to the condition of fluid flow is laminar in natural convection. Grashof number is applied to determine the flow field behavior around a heat sink. The heat sink material is aluminum and the density of air depends on Boussinesq approximation.

The validation result needed to be studied to compare the numerical results against the experimental results. The validation result is an important result for further study of the suitable geometry of heat sink in heat transfer performance.

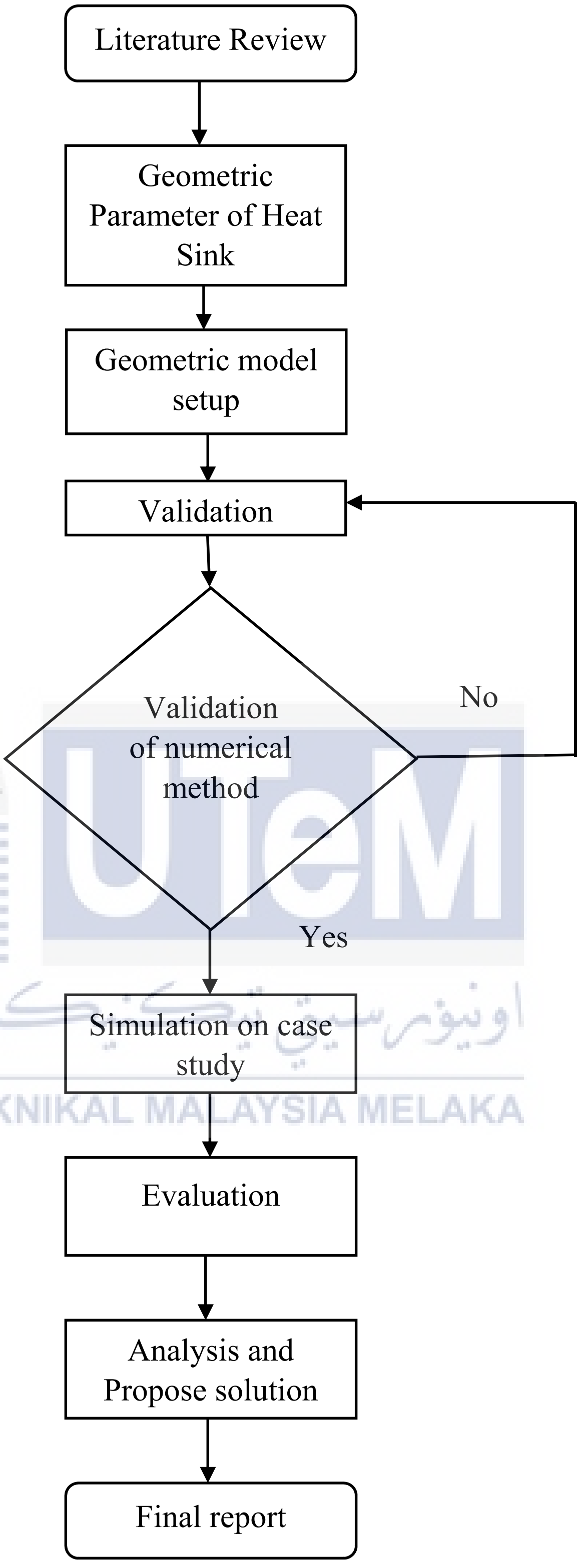




Figure 3.1: The Methodology Flowchart.

## 3.2 Geometric Model (Reference)

To validate the results, it is necessary to refer to the geometry parameters of reference heat sink. As shown in Figure 3.2 (b), the computational domain is set to 3L/4 for fin length, 9H for fin height, and S/2 for fin spacing. The geometry parameters of reference heat sink as shown in Table 3.1.

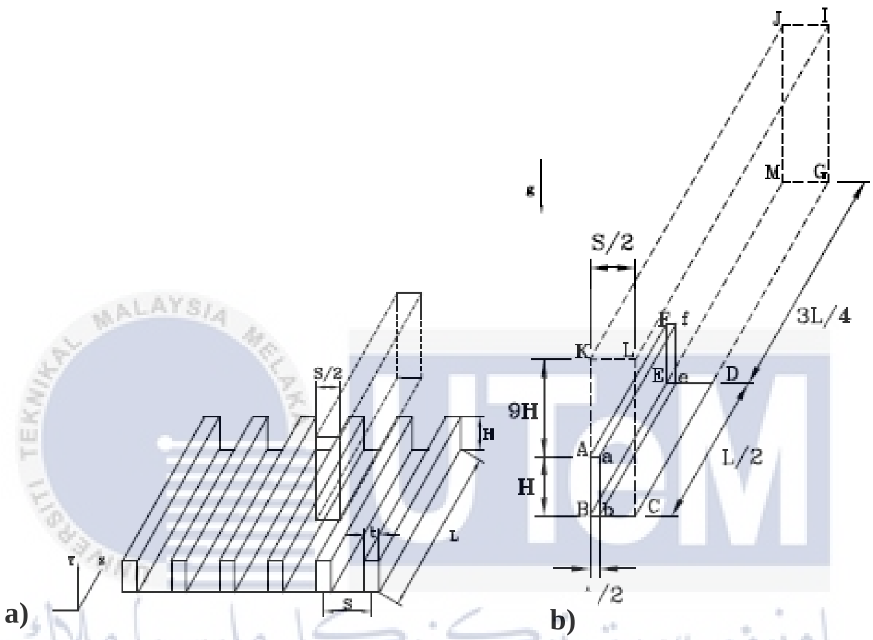


Figure 3.2: (a) Drawing of fin arrays and (b) Computational domain (Dialameh et. al. 2018).



Table 3.1: The geometric parameters of references heat sink.

| Parameters | Value |
|---|---|
| Fin length, L | 127 mm |
| Fin height, H | 38 mm |
| Fin spacing, S | 6.3 mm |
| Fin thickness, t | 1.27 mm |
| Number of spacing in fin arrays, n | 33 |
| Computational domain of fin length | 3L/4 |
| Computational domain of fin height | 9H |
| Computational domain of fin spacing | S/2 |

## 3.3 Boundary Conditions

In this project, the computational domain as shown in Figure 3.3, where ABbaCDdc is a one-quarter of the total fin array. The constant temperature, $T_b$ is set at the base surface, BbDd. The two side wall surface is set as symmetry boundary condition where the wall surface ABCD and ACDEFG for x = 0 plane and ABab and AabKHGA for z = 0 plane. There are three inlets of air assumed at KJHI and JEIF in the back and KJEDdbB in the bottom. Whereas, there is one air outlet assumed at GFHI in the top of the fin arrays.

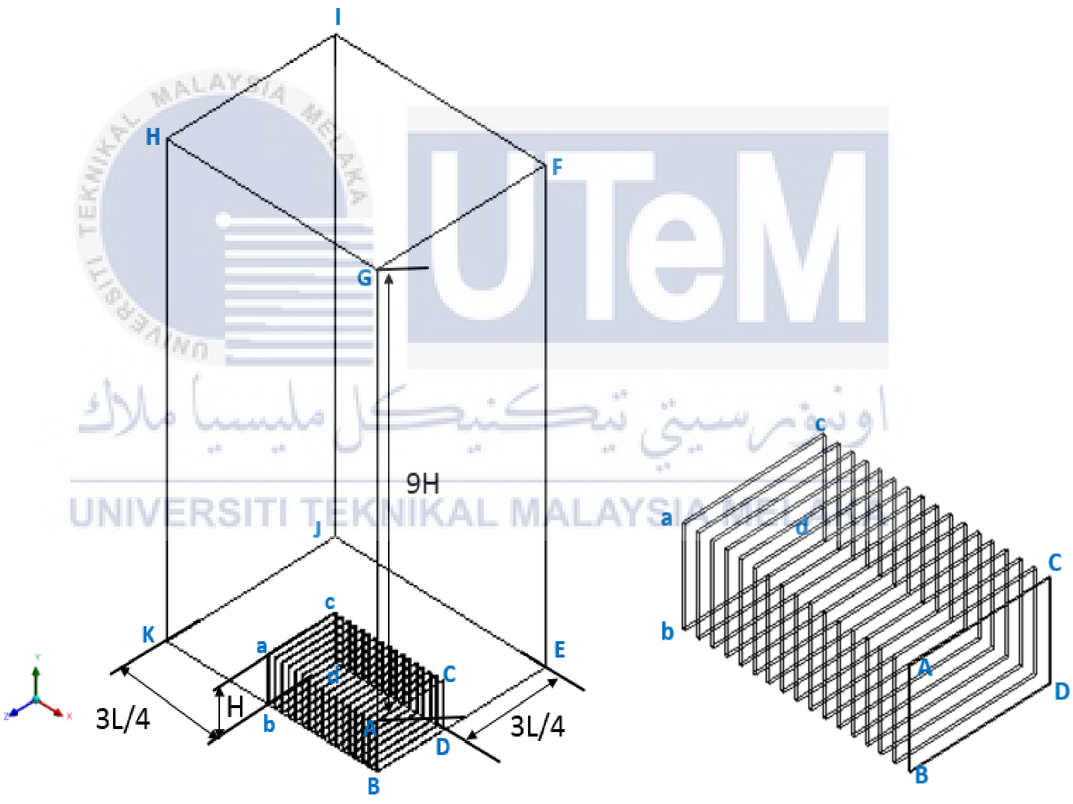


Figure 3.3: Computational domain and Schematic drawing of fin arrays.

## 3.4 Physical properties of flow

Generally, a heat sink performance is usually dependent on the material of heat sink used and airflow. Aluminum alloys are the most common material used for the heat sink. The density of air depends on the Boussinesq approximation. Table 3.2 showed the physical properties of aluminum and air used for the study of validation results.

Table 3.2: Physical properties of Aluminum and Air.

| **Physical Properties** | **Aluminum** | **Air (Boussinesq)** |
|---|---|---|
| Density (kg/$m^3$) | 2719 | 1.204 |
| Thermal conductivity, k (W/m.K) | 202.4 | 0.0242 |
| Specific heat (J/Kg.K) | 871 | 1006.43 |
| Viscosity (Kg/m.s) | - | 1.7894 x $10^{-05}$ |
| Thermal Expansion Coefficient (1/K) | - | 0.00343 |



## 3.5 Meshing strategy

The computational domain is divided into simple elements by using the meshing process. The mesh influences the convergence, accuracy and simulation precision. Therefore, it is important to have a good strategy in meshing in to obtain faster and more accurate of the solution. In this domain, the tetrahedral mesh cells are formed by using different types of meshing.

There were five meshing strategies applied in this computational analysis domain. First, the edges sizing was applied at domain and fin arrays as shown in Table 3.3. The edges sizing at a domain is to reduce the number of sizes for better simulation.

The edges sizing at fin arrays is to analyze the flow field pattern over the fin arrays and to further study the effect of different height of fin.

Table 3.3: Edges sizing setting

<table>
<tr><th colspan="2">Domain</th><th colspan="2">Fin arrays</th></tr>
<tr><td>Geometry</td><td>9 Edges</td><td>Geometry</td><td>204 Edges</td></tr>
<tr><td>Element size</td><td>24 mm</td><td>Element size</td><td>1.6 mm</td></tr>
<tr><td>Behaviour</td><td>Hard</td><td>Behaviour</td><td>Hard</td></tr>
<tr><td colspan="2">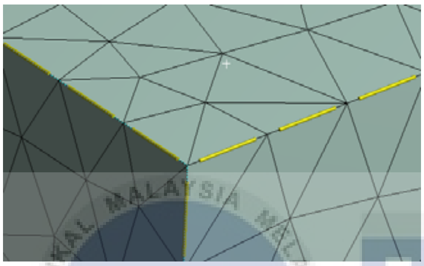<br>Figure 3.4: Edge sizing for domain</td><td colspan="2">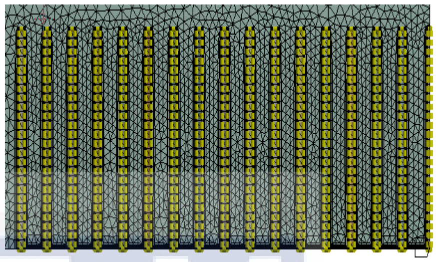<br>Figure 3.5: Edge sizing for fin arrays</td></tr>
</table>

Second, five inflation layer are set to the boundary layer of the fin arrays to capture the boundary layer effects. Table 3.4 showed the inflation setting. The inflation was applied around the fin arrays as shown in Figure 3.6.



Table 3.4: Inflation setting.

<table>
<tr><td>Geometry</td><td>18 Bodies</td><td rowspan="6">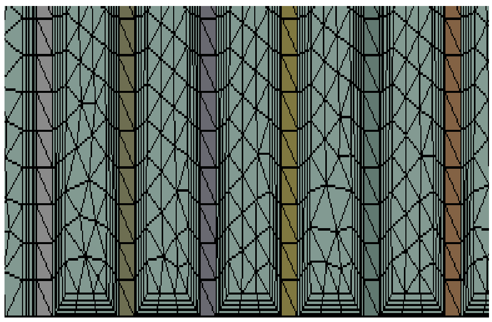<br>Figure 3.6: Inflation layer</td></tr>
<tr><td>Boundary</td><td>118 Faces</td></tr>
<tr><td>Inflation option</td><td>First layer thickness</td></tr>
<tr><td>First layer height</td><td>0.16 mm</td></tr>
<tr><td>Maximum layer</td><td>5</td></tr>
<tr><td>Growth rate</td><td>1.15</td></tr>
</table>

The face sizing for fin arrays is to increase the number of nodes in the triangular cell. The more nodes in the tetrahedral cell will show a more accurate result of the fluid flow pattern. Table 3.5 showed the face sizing setting for fin arrays.

Table 3.5: Face sizing setting.

<table>
<tr><td>Geometry</td><td>34 Faces</td><td rowspan="3">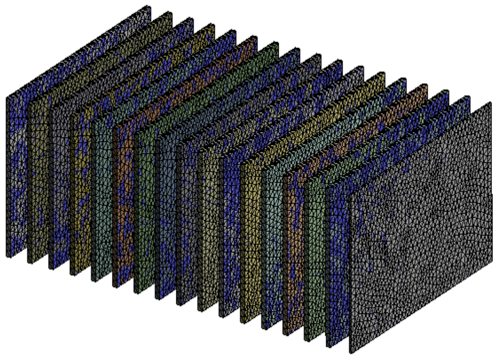<br>Figure 3.7: Face sizing for fin arrays.</td></tr>
<tr><td>Element size</td><td>1.6 mm</td></tr>
<tr><td>Behaviour</td><td>Hard</td></tr>
</table>

The body sizing is to increase the number of elements around the fin arrays. It is important to study flow field patterns over the fin arrays due to natural convection current may occurs in the heat sink. Table 3.6 showed the body sizing setting.

Table 3.6: Body sizing setting.

<table>
<tr><td>Geometry</td><td>1 Body</td><td rowspan="6">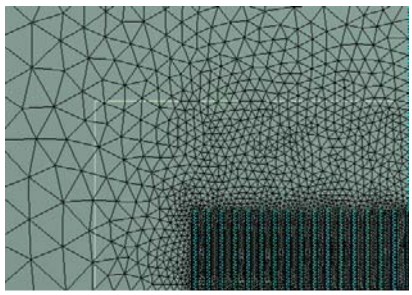<br>Figure 3.8: Body sizing.</td></tr>
<tr><td>Type</td><td>Body of Influence</td></tr>
<tr><td>Bodies of Influence</td><td>1 Body</td></tr>
<tr><td>Element size</td><td>4.0 mm</td></tr>
<tr><td>Growth rate</td><td>1.150</td></tr>
<tr><td>Local min size</td><td>0.2282 mm</td></tr>
</table>

The domain is divided into 1244068 tetrahedron elements as shown in Figure 3.9.

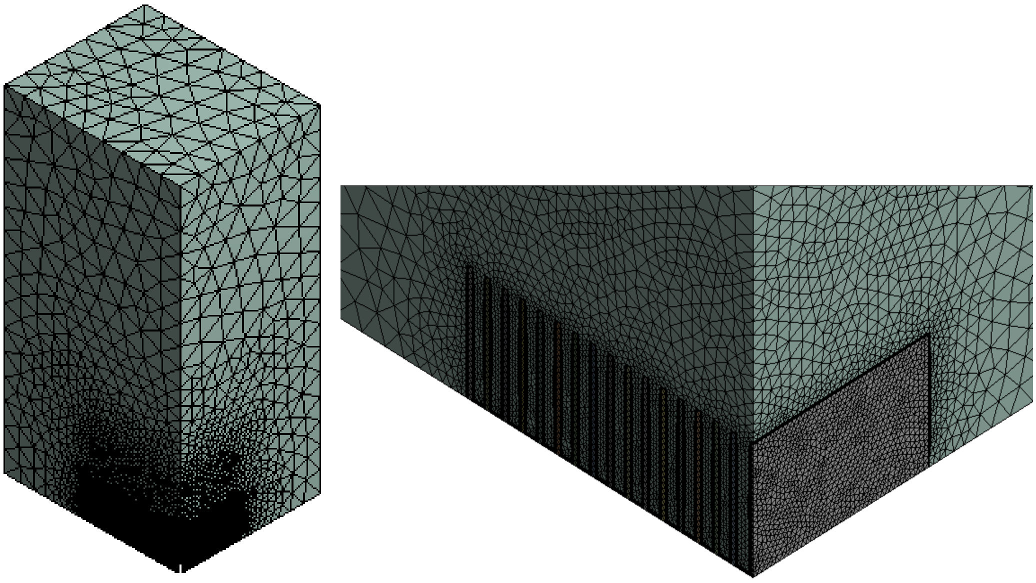

Figure 3.9: The meshing result.

## 3.6 Governing Equations

The physical properties of fluid and solid will be described by using governing equation of computational fluid dynamics. The governing equation will then be translated to discretized form and solve by Ansys software.

### 3.6.1 Governing equations for air

Continuity equation:

$$\frac{\partial(\rho u)}{\partial x} + \frac{\partial(\rho v)}{\partial y} + \frac{\partial(\rho w)}{\partial z} = 0$$

where $\rho$ is the density (kg/$m^3$), u is the x-component of velocity (m/s), v is the y-component of velocity (m/s) and w is the z-component of velocity (m/s).

Momentum equations:

$$\frac{\partial(\rho u^2)}{\partial x} + \frac{\partial(\rho uv)}{\partial y} + \frac{\partial(\rho uw)}{\partial z} = - \frac{\partial P}{\partial x} + \mu(\frac{\partial^2 u}{\partial x^2} + \frac{\partial^2 u}{\partial y^2} + \frac{\partial^2 u}{\partial z^2})$$

$$\frac{\partial(\rho vu)}{\partial x} + \frac{\partial(\rho v^2)}{\partial y} + \frac{\partial(\rho vw)}{\partial z} = - \frac{\partial P}{\partial y} + \mu(\frac{\partial^2 v}{\partial x^2} + \frac{\partial^2 v}{\partial y^2} + \frac{\partial^2 v}{\partial z^2}) + g(\rho - \rho_a)$$

$$\frac{\partial(\rho wu)}{\partial x} + \frac{\partial(\rho wv)}{\partial y} + \frac{\partial(\rho w^2)}{\partial z} = - \frac{\partial P}{\partial x} + \mu(\frac{\partial^2 w}{\partial x^2} + \frac{\partial^2 w}{\partial y^2} + \frac{\partial^2 w}{\partial z^2})$$

where $\rho$ is the density (kg/$m^3$), P is the pressure (Pa), u is the x-component of velocity (m/s), v is the y-component of velocity (m/s), w is the z-component of velocity (m/s), g is the gravity and μ is the dynamic viscosity, N/$m^2$s.

Energy equation:

$$\frac{\partial(\rho uT)}{\partial x} + \frac{\partial(\rho vT)}{\partial y} + \frac{\partial(\rho wT)}{\partial z} = \frac{k}{c_p}(\frac{\partial^2 T}{\partial x^2} + \frac{\partial^2 T}{\partial y^2} + \frac{\partial^2 T}{\partial z^2})$$



where $\rho$ is the density (kg/$m^3$), u is the x-component of velocity (m/s), v is the y-component of velocity (m/s), w is the z-component of velocity (m/s), T is the temperature in °C and $c_p$ is the coefficient of heat capacity, J/(kg°C).

### 3.6.2 Governing equations for fin arrays

Fourier's law of heat conduction equation:

$$(\frac{\partial^2 T}{\partial x^2} + \frac{\partial^2 T}{\partial y^2} + \frac{\partial^2 T}{\partial z^2}) = 0$$

where T is the temperature in °C

## 3.7 Fluent Model

Ansys fluent simulation tool is used to solve the numerical result. In this study, a heat sink is located in a fluid domain with three inlets and one outlet. The boundary conditions for inlet and outlet are changed to pressure inlet and outlet with gauge pressure equal to zero. For the inlet, set the total temperature to 20℃ as ambient temperature. For the outlet, set the backflow total temperature to 20℃ as well. The average heat transfer coefficient of the heat sink will be evaluated under various temperature differences, $\Delta T$ between 33 and 85 K at $T_a$ = 293 K as ambient temperature. Three different value of constant temperature, $T_b$ (53, 75 and 105 °C) is set at the base surface of the heat sink.

The average heat transfer coefficient is defined as:

$$h = \frac{Q}{A\Delta T}$$

where Q is the total heat transfer rate from fin arrays to the surrounding, A is the total heat transfer area of the fin arrays and $\Delta T$ is the temperature difference between the base surface and ambient air, $(T_b - T_a)$.



The viscous laminar model is applied to the heat sink due to the condition of fluid flow is laminar in natural convection. The behavior of fluid flow depends on the Grashof number, where the boundary layer is laminar that is in the range of $10^3 < Gr_H < 10^6$.

The Grashof number is defined as:

$$Gr_H = \frac{g\beta\Delta T H^3\rho^2}{\mu^2}$$

where g is the gravity, $\beta$ is the coefficient of thermal expansion, $\Delta T$ is the temperature difference between the base surface and ambient air, H is the fin height, $\rho$ is the density and $\mu$ is the coefficient of viscosity.

The implicit finite element method will be applied for simulate the flow fluid pattern with coupled temperature and velocity. The governing equations were solved by using the SIMPLE algorithm. The convective and diffusive terms of governing equations were discretized by two schemes which are the upwind and central difference schemes.

There was a difficulty for the continuity equation to converge when running the calculation. For the solution to converge, it is necessary to change the property of air at the setup of materials. The density of air is changed to Boussinesq approximation as shown in Table 3.2.

### 3.8 Grid Dependency Test

In this section, several mesh sizes were made to obtain the accuracy of stimulated results that is constant average heat transfer coefficient and flow field. Different mesh sizes will gain a different numerical result. As shown in Figure 3.10, the gap between the medium grid case and fine grid case was very close as compared to the gap between coarse and medium grid cases. This indicated that there is a small difference in a stimulated result between the medium grid case and the fine grid case. Thus, a heatsink with a mesh size of 776268 was selected to run the simulation.

Table 3.7: Grid Dependency Test.

| **Grid Type** | **Coarse** | **Medium** | **Fine** |
|---|---|---|---|
| **Mesh Size** | 482070 | 776268 | 1244068 |
| **Average Heat Transfer Coefficient, h (W/$m^2$.K)** | 4.69 | 4.80 | 4.85 |
| **Percentage Error, %** | 5.44 | 3.23 | 2.27 |

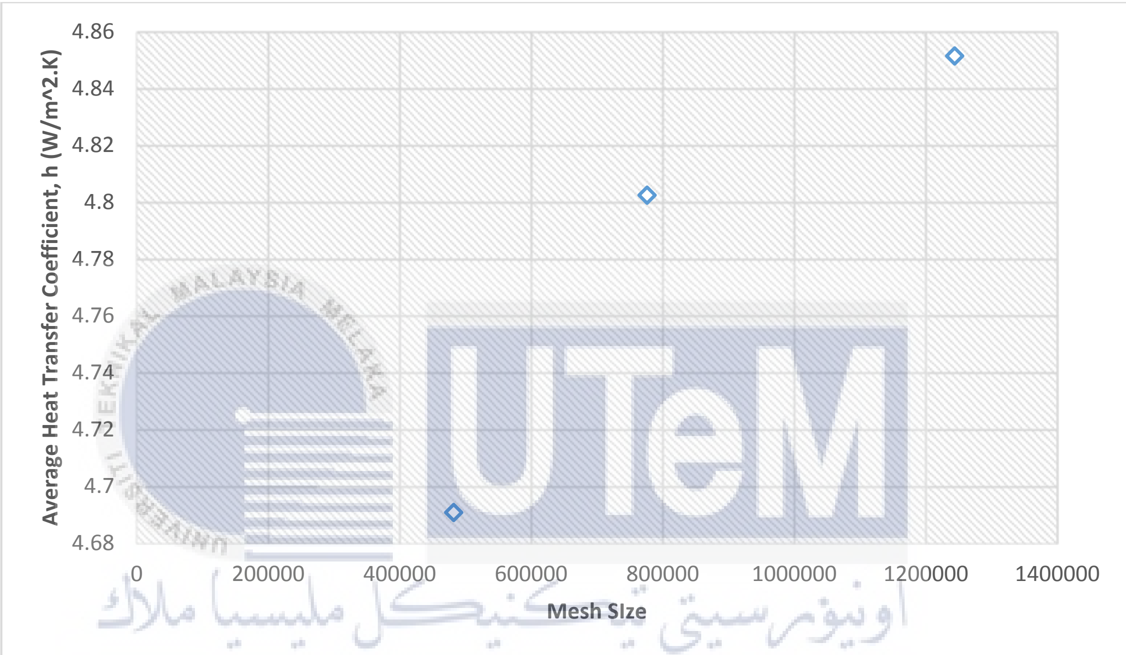




Figure 3.10: The three different grid test towards average heat transfer coefficient.

## 3.9 Validation

The variation of average heat transfer coefficient, h with temperature difference,$\Delta T$ between 33 and 85 $K$ as shown in Figure 3.11. The graphical result showed the result of a comparison between the experimental results (Harahap & McManus and Dialameh) and numerical result. As shown in Figure 3.11, the numerical result was in the same order with the experimental result. Thus, it is confirmed that the fluent setting for numerical analysis able to simulate a horizontal rectangular heatsink under natural convection flow.

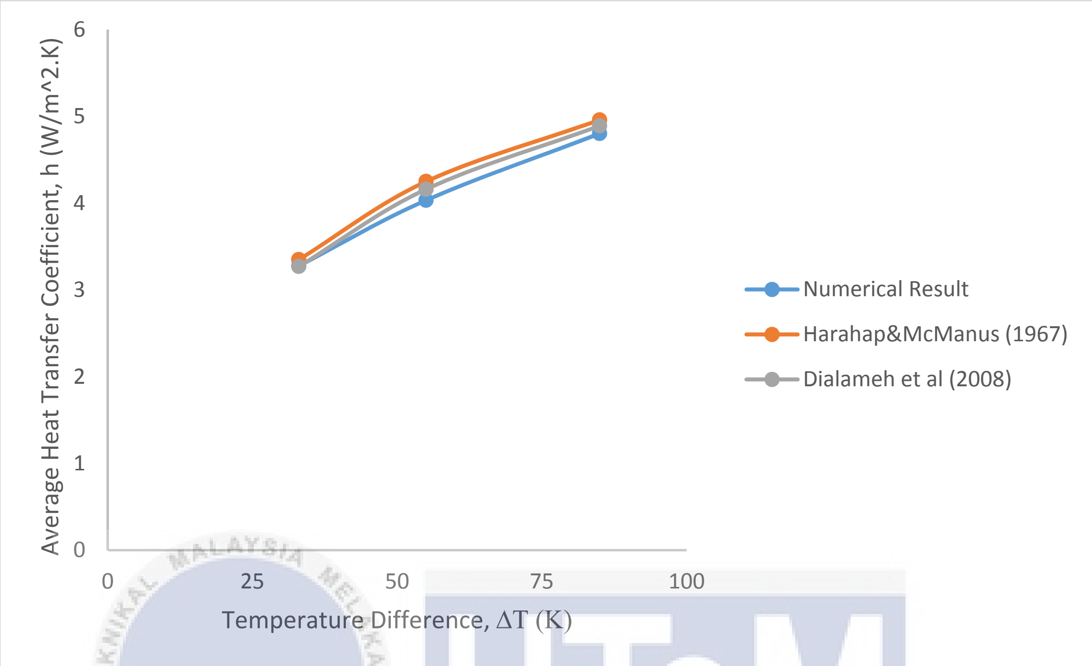


Figure 3.11: The graph of variation of average heat transfer coefficient, h with temperature difference, $\Delta T$.



## 3.10 Ansys Model Generation

With the valid result between the numerical and experimental data, two different models of fin geometries (Concave model and Convex model) were constructed to compare with the Flat model. The geometric parameters of Flat model are n = 8, S = 6.35 mm, th = 1.27 mm, H = 38.1 mm and L = 63.5 mm as shown in Figure 3.9.1(a). The shape of each fin in the Flat model is arranged horizontally without experience various fin height materials distribution.

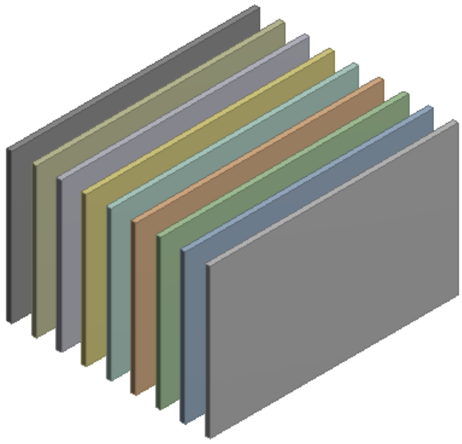

(a) Flat model.

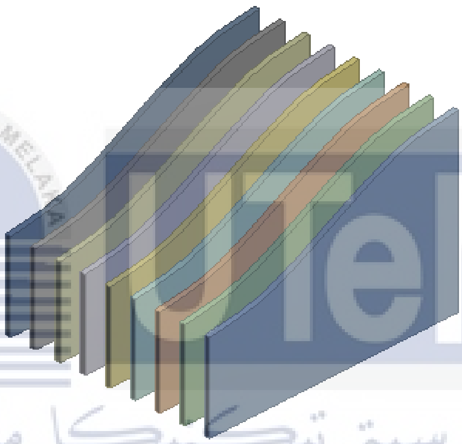

(b) Convex model



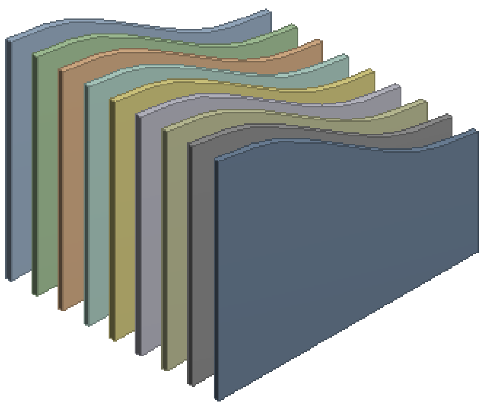

(c) Concave model

Figure 3.12: Fin array configuration.

The Concave and Convex models are constructed by following the shape of the cosine curve that showed in Figure 3.13. The shape of each fin in Convex and Concave models are arranged sinusoidally along the fin length direction, as illustrated in Figure 3.12 ((b) and (c)). The increase or decrease of fin mass in the formulated direction will experience various fin mass distribution under the constraint of a fixed mass of fin material. The equation that describes the shape of the cosine curve for three different models is defined as follows.

$$H = Mcos(2\pi f L)$$

where H is the fin height, M is the amplitude of the cosine graph, f is the frequency of cosine function and L is the length of fin. The amplitude of the cosine graph, M is used to control the amount of increase or decrease in fin mass distribution.

In this study, the average heat transfer coefficient will be calculated under constant fin length, L = 63.5 mm, constant fin thickness, th = 1.27 mm and various temperature differences between 33 and 85 K. The height of the fin will be varied by following the equation of cosine curve shape to achieve the objective of the study.



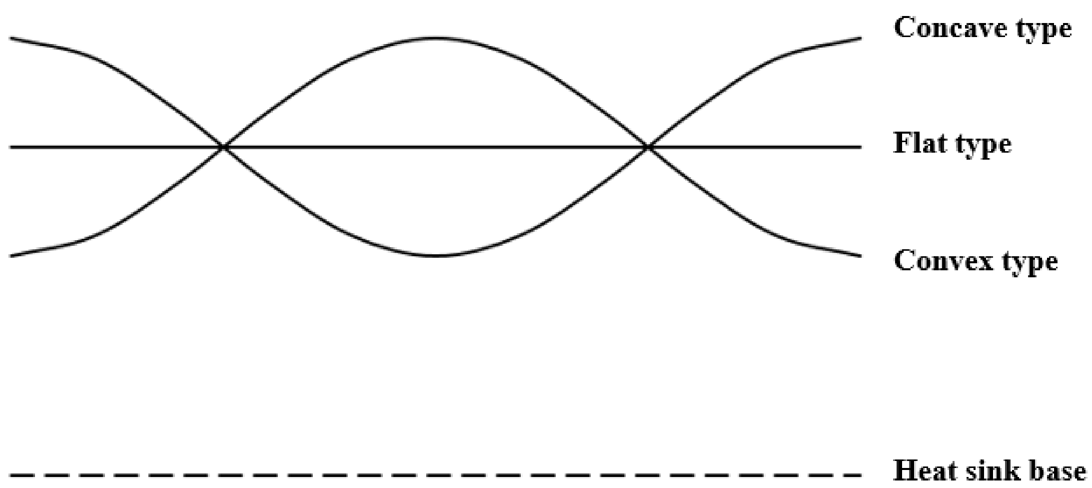


Figure 3.13: Shape of the cosine curve.

### 3.11 Central Composite Design (CCD) For Geometric Optimization

In this section, a geometric optimization that uses Central Composite Design (CCD) will be discussed. An optimization is performed to obtain the optimal settings for two factors: fin height, ($X_1$ = H) and heat sink base thickness, ($X_2$ = $t_b$). These two factors will affect the average heat transfer coefficient. The aim is to determine the optimal settings of two factors that can maximize the average heat transfer coefficient.

The three-level factorial design with two factors is used in Central Composite Design. Thus, this design will required nine runs ($3^2$ = 3 x 3 = 9). A Central Composite Design with three-level, two factor factorial design is shown in Table 3.8.

Table 3.8: A Central Composite Design with three-level, two factor factorial design.

| Experiment runs | Factor $X_1$ | Factor $X_2$ |
|---|---|---|
| 1 | -1 | -1 |
| 2 | 1 | -1 |
| 3 | -1 | 1 |
| 4 | 1 | 1 |
| 5 | -1.414 | 0 |
| 6 | 1.414 | 0 |
| 7 | 0 | -1.414 |
| 8 | 0 | 1.414 |
| 9 | 0 | 0 |



From the above table, the CCD consists of four factorial runs, four axial runs and one center point run. In this design, the low and high values for factor $X_1$ and $X_2$ are represented as -1 and 1, and the intermediate value as 0. The axial point value depend on alpha, $\alpha$ ($\alpha = sqrt$ $(2)$ = 1.414).

# CHAPTER 4

# RESULTS AND DISCUSSION

## 4.1 Introduction

In this chapter, the selection of the optimum model will be discussed. To select the optimal configuration of fins, three different types of the heatsink (Flat, Convex, and Concave models) were compared. The effect of changing fin height with a fixed mass of fin material toward the average heat transfer coefficient will be performed. The design optimization for the average heat transfer coefficient was conducted with various fin height and heat sink base thickness by using the CCD (Central Composite Design) method.

## 4.2 Comparison of the Flat, Convex and Concave models

The hotter heat flow enters into the bottom part of the heat sink and flows up to the colder upper part of the heat sink. The ambient air flows into the inner part of the heat sink causing the temperature of the fin near the outside region to decrease. Figure 4.1 shows the heat sink surface temperature distributions on the heat sink wall, to compare the Flat, Convex, and Concave models.

As observed in Figure 4.1, the highest temperature distribution occurs in the base surface of the heat sink and with furthering increasing the fin mass distribution near the outer region, the temperature gets lower. The maximum temperature of the heat sink is inversely proportional to the fin mass distribution near the outer region.

The bigger the fin mass distribution near the outer region causes the lower the maximum temperature of the heat sink.

As Figure 4.1(c) indicates, the Concave model has a lower maximum temperature because it has a bigger fin mass distribution near the outer region. Figure 4.1(b) indicates, for the Convex model, the temperature of fin materials is mostly held at high temperatures when the colder ambient air rises over the rectangular fin arrays, due to the decreasing of fin mass near the outer region of the heat sink. This indicated that the bigger the fin mass near the outer region, the larger the surface area and thus the heat transfer rate gets higher.

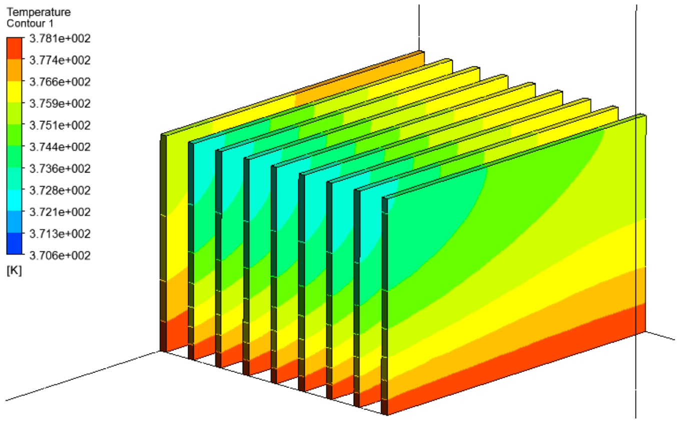


a) Flat type

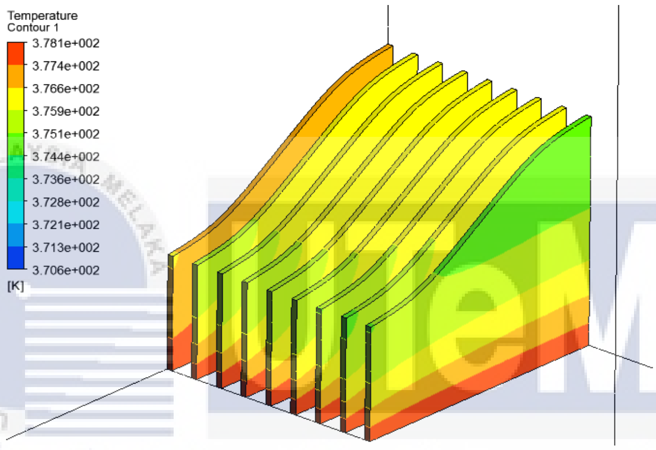


b) Convex type



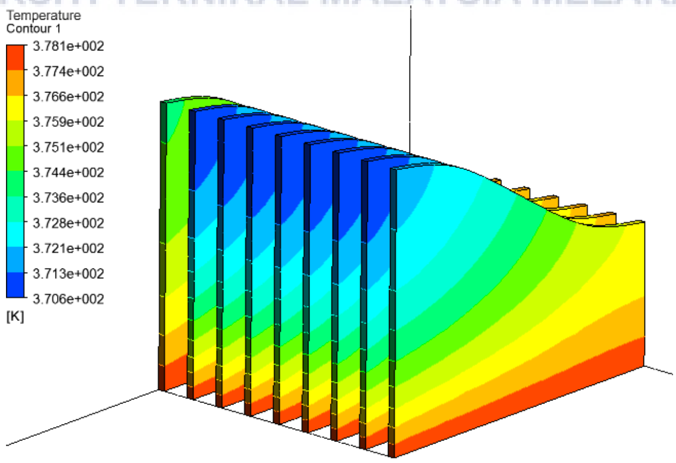


c) Concave type

Figure 4.1: Heat sink surface temperature distributions. (n = 8, S = 6.35mm, th = 1.27mm, L =63.5mm and $\Delta T$ = 85 K)

## 4.3 Flow Field Observations

As observed in Figure 4.2, the flow pattern is basically of a single chimney type (Dialameh et al, 2008). The chimney effect occurs when fresh cool air enters from the outside region of the heat sink, absorbs heat in the fin array and then flows upward along with the height of the fin.

Figure 4.2(c) indicates, for the Concave model, the thermal boundary layer is thicker among the three models. This can be justified by the longer fin near the outer side able to receive a larger mass flow rate of fresh air from the surrounding air. Due to the rate of the natural convection heat transfer is directly related to the mass flow rate of the fluid. Therefore, the larger mass flow rate of fresh air can lead to a higher natural convection heat transfer rate. Besides, the natural convection current is formed by the dynamic balance of buoyancy and friction effect. The buoyancy force is induced due high temperature difference are introduced on the fin surfaces. Figure 4.2(b) indicates, for the Convex model, the friction force increases because the more fin mass distribution is introduced in the inner region of the heat sink, and thus disrupting the fluid flow and heat transfer. As a result, decreasing the fin height from the outer region to the inner region of the heat sink can enhance natural convection current.

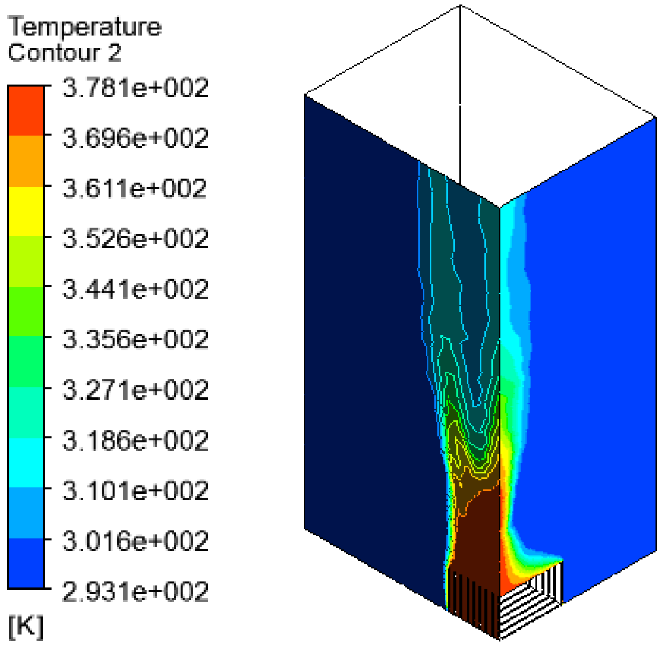


(a) Flat type.

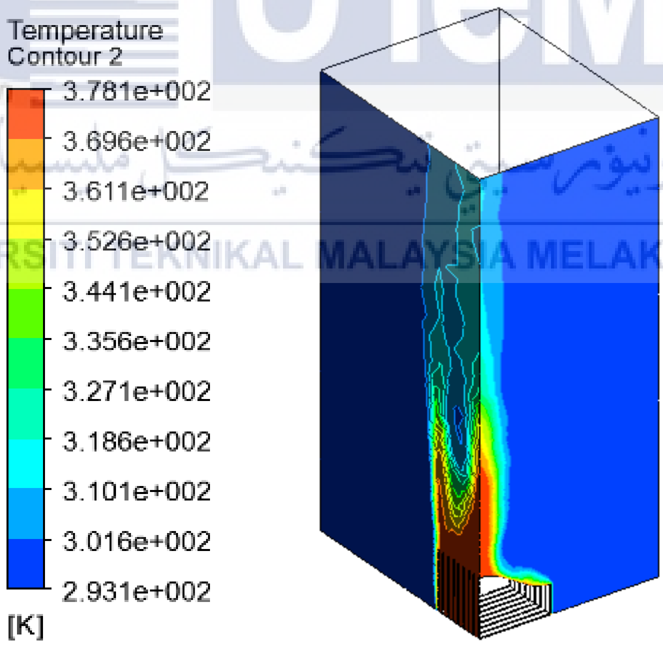


(b) Convex type.

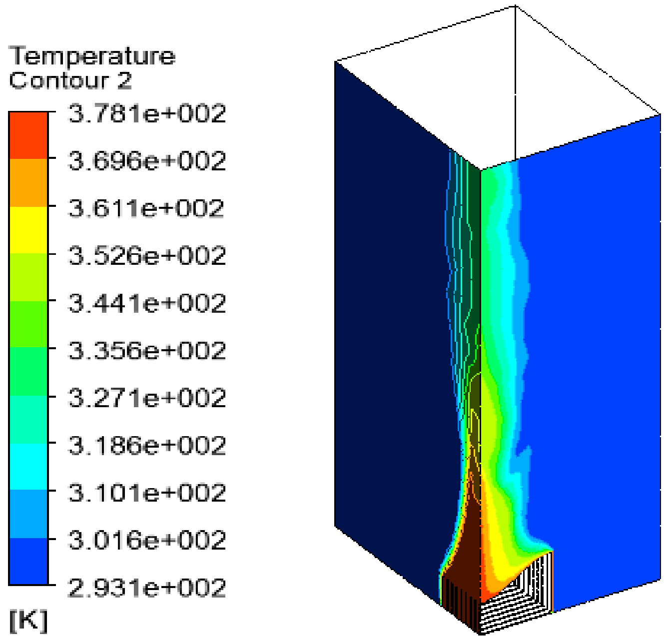


(c) Concave type.

Figure 4.2: Temperature distributions on the symmetry wall, $\Delta T$ = 85 K.

Table 4.1: Numerical result of three different models.

| Temperature Difference, $\Delta T\ (K)$ | Average Heat Transfer Coefficient, h $(W/m^2K)$ | | | Increment percentage, % | |
|---|---|---|---|---|---|
| | Flat **(reference)** | Convex | Concave | Flat/ Convex | Flat/ Concave |
| 33 | 3.70 | 2.64 | 4.56 | -28.65 | 23.24 |
| 55 | 4.45 | 3.25 | 5.35 | -26.97 | 20.22 |
| 85 | 5.10 | 4.00 | 6.14 | -21.57 | 20.39 |

From table 4.1, the average heat transfer coefficient increases with increasing temperature differences. As observed, more than 20% of improvement in the average heat transfer coefficient for the Concave model as compared to the Flat model. Whilst, there is a decrease of more than 20% in the average heat transfer coefficient for the Convex model as compared to the Flat model.

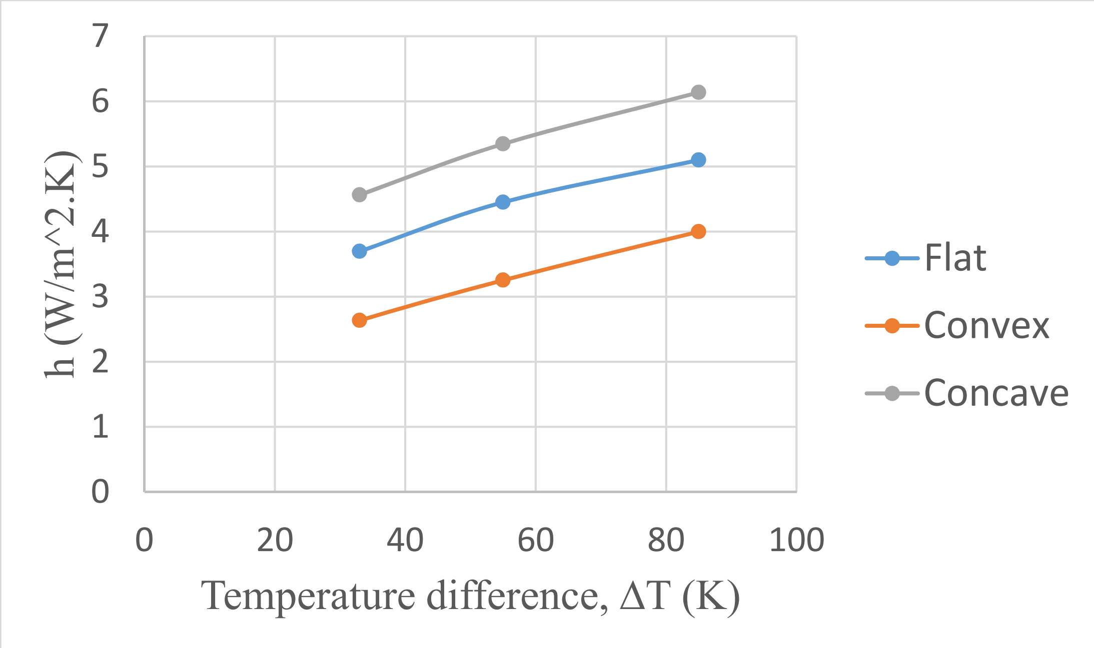


Figure 4.3: Averaged heat transfer coefficient as a function of base temperature difference.

As shown in Figure 4.3, the average heat transfer coefficient increases with increasing temperature difference. When the fin mass decreases near the outside region, the heat transfer performance will be degraded. This is because of the smaller mass flow rate of fresh air from the surrounding air and smaller heat transfer area near the outer side are introduced on the heat sink. Besides, the air density decreases with the increasing temperature difference in natural convection heat transfer. Hence, the buoyancy force is induced due to the higher temperature difference. By comparing the average heat transfer coefficient of the three models, the Concave model is selected as the optimal configuration of fins, because it exhibited the highest heat transfer coefficient.

## 4.4 Optimization

To maximize an average heat transfer coefficient, the design parameters are selected as the fin height ($X_1$ = H) and heat sink base thickness ($X_2$ = $t_b$). The optimization was performed concerning temperature difference, ΔT = 85 K, the number of spacing in fin array, n = 8, fin spacing, S = 6.35 mm, fin thickness, th = 1.27 mm and fin length, L = 63.5 mm by using a statistical software package (Minitab). By using CCD (Central Composite Design), nine experimental runs are chosen for geometry optimization to produce a response surface, as shown in Table 4.2. Thus, the response surface was generated according to the experimental point by using Ansys fluent simulation tool. The optimization will then performed to obtain the optimal value of $X_1$ and $X_2$, using a statistical software package (Minitab). The Design of Experimentations (DOE) in Minitab in this research is used to identify the relationship between two factors in maximizing the response.



Table 4.2: Design of experiment. (n = 8, S = 6.35mm, th = 1.27mm, L =63.5mm and ΔT = 85 K)

| Experiment runs | Parameters | | Response |
|---|---|---|---|
| | $X_1$ | $X_2$ | h (W/$m^2$K) |
| 1 | 25.4000 | 2.000 | 8.239 |
| 2 | 50.8000 | 2.000 | 10.105 |
| 3 | 25.4000 | 6.000 | 8.878 |
| 4 | 50.8000 | 6.000 | 10.403 |
| 5 | 20.1422 | 4.000 | 7.542 |
| 6 | 56.0578 | 4.000 | 10.124 |
| 7 | 38.1000 | 1.172 | 9.687 |
| 8 | 38.1000 | 6.828 | 10.050 |
| 9 | 38.1000 | 4.000 | 10.024 |

Table 4.3 shows the result of $X_1$ and $X_2$ settings for producing the maximum response of the average heat transfer coefficient, h. In Figure 4.4, which plots the average heat transfer coefficient for the rectangular fin against the fin height and heat sink base thickness, the maximum h of 10.4136 W/$m^2$K, was detected at a fin height of 46.6254 mm and heat sink base thickness of 5.9710 mm.

Table 4.3: Statistical result of Minitab.

| **Parameters** | | **Response** |
|---|---|---|
| $X_1$ | $X_2$ | **h (W/$m^2$K)** |
| 46.6254 | 5.9710 | 10.4136 |

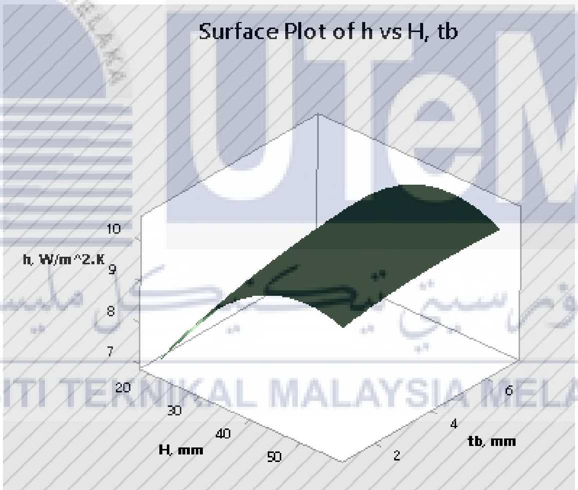


Figure 4.4: Surface plot of h versus H, $t_b$.

To validate the accuracy of the result, a fin geometry was constructed based on the optimal value of fin height and base thickness obtained from response optimization. The optimal geometry parameters are n = 8, S = 6.35 mm, th = 1.27mm, L =63.5mm, H = 46.6254 mm and $t_b$ = 5.9710 mm, as shown in Figure 4.5. The average heat transfer coefficient was evaluated through numerical analysis and the result obtained as 10.3710 W/$m^2$K. The percentage error between the statistical result and the numerical result shows 0.41%, indicating a good agreement. Therefore, this result implies that it can optimize the average heat transfer coefficient concerning fin height and heat sink base thickness.

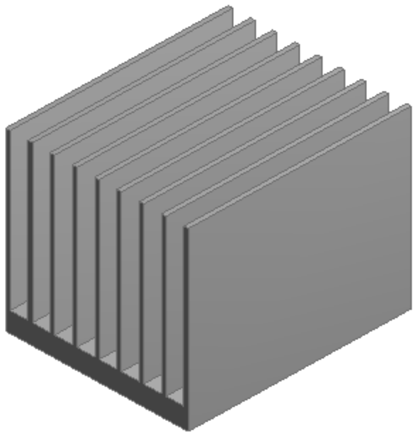

Figure 4.5: Optimum design of horizontal rectangular heat sink with base.

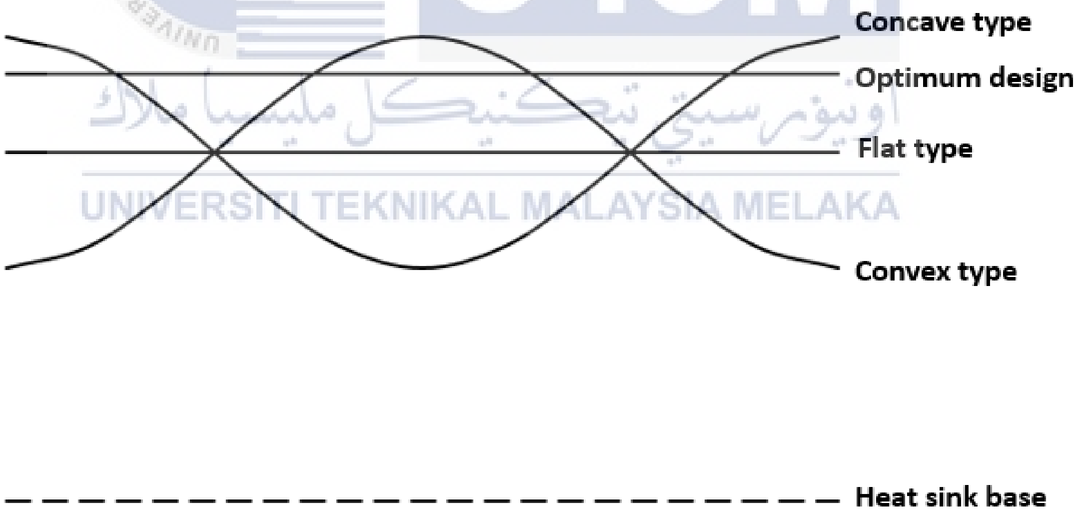


Figure 4.6: Comparison of optimum design with three different models.

# CHAPTER 5

# CONCLUSION AND RECOMMENDATIONS

In this research, numerical simulations were performed to optimize a horizontal rectangular heat sink for LED lighting. The values of the average heat transfer coefficient were calculated for three different models: Flat, Convex, and Concave models. Three types of heat sink (Flat, Convex, and Concave models) were compared in order to select the optimum configuration of fin. An optimum heat sink model, the Concave model, without increasing the cost of production was obtained through simulation performed by Ansys software. In summary, the value of the average heat transfer coefficient for the Concave model was found to be higher among the three models.

The effect of fin mass distribution across the heat sink under the constraint of a fixed mass of fin material towards the average heat transfer coefficient was performed. As the fin mass distribution near the outer side increases, the average heat transfer coefficient also increases. It was found that the bigger fin mass near the outer region able to receive a larger mass flow rate of fresh air from the ambient air. Besides, it was also found that the bigger fin mass distribution in the inner region able to increase the friction force, and thus slowing down the fluid flow and heat transfer rate. Hence, decreasing the fin mass distribution from the outer side to the inner side of the heat sink can enhance the natural convection current. Finally, the heat sink geometry with a heat sink base was optimized using a CCD (Central Composite Design). The result implies that it can optimize the average heat transfer coefficient by concerning various fin height and heat sink base thickness.

The simple shape of a heat sink (Flat type) was usually used in LED lighting. But, they have the limit of cooling performance. The flow of fresh air is greatly impacted by the arrangement of fins on a heat sink. The configuration of fins must be optimized to allow more fresh air to go through a heat sink. Therefore, there are some suggestions for research arising from this work. Various fin shapes needed to be studied to enhance cooling performance. More fin mass distribution must be added near the outer region and lesser fin mass distribution must be introduced in the inner region of the heat sink to promote the fluid flow and heat transfer as shown in this research.

## REFERENCES


Hwan Yu, S., Soo Lee, K., and Jin Yook, S. (2011) Optimum design of a radial heat sink under natural convection. *International Journal of Heat and Mass Transfer*, 17: 133-791.

Shah, A., Sammakia, B.G., Srihari, K., and Ramakrishna, K. (2006) Optimization Study for a Parallel Plate Impingement Heat Sink. *Journal of Electronic Packaging*, Vol 128: 311-318.

Bello-Ochende, T., Meyer, J.P., and Bejan, A. (2010) Constructal multi-scale pin-fins. *International Journal of Heat and Mass Transfer*, 53: 2773-2779.

Ahmed, H.E., Salman, B.H., Kherbeet, A.S., and Ahmed, M.I. (2018) Optimization of thermal design of heat sinks: A review. *International Journal of Heat and Mass Transfer*, 118: 129-153.

Khattak, E.Z., Ali, H.M., Ahmad, E.J., and Shah, E.S. (2016) PLATE FIN AND PIN FIN HEAT SINK VARIOUS DESIGN ASPECTS, (REVIEW ON HEAT SINK COMPETENCE). Retrieved from https://www.researchgate.net/publication/309390235

H.Y. Li, M.H. Chiang, C.I. Lee, W.J. Yang. (2010) Thermal performance of plate-fin vapour chamber heat sinks, Int. Commun. *Heat Mass Transf*. 37 (7):731–738.

L. Dialameh, M. Yaghoubi, and O. Abouali. (2008) Natural convection from an array of horizontal rectangular thick fins with short length. *Applied Thermal Engineering*, 28: 2371-2379.

F. Harahap, and H. N. McManus, JR. (1967) Natural Convection Heat Transfer From Horizontal Rectangular Fin Arrays. *Transaction of the ASME*, pp. 32-38.

K. E. Starner and H. N. McManus, JR. (1963) An Experiment Investigation of Free-Convection Heat Transfer From Rectangular-Fin Arrays. Journal of Heat Transfer, pp. 273-277.

E. Z. Khattak, H. M. Ali, E. J. Ahmad and E. S. Shah. (2016) Plate Fin And Pin Fin Heat Sink Various Design Aspects. Research Gate.

H. E. Ahmed, B. H. Salman, A. Sh. Kherbeet and M. I. Ahmed. (2018) Optimization of thermal design of heat sinks. International Journal of Heat and Mass Transfer. 118: 129-153.

J.R. Pryde, D.C Whalley, 2014. A review of LED technology trends and relevant thermal management strategies, in: Presented at the 14th IEEE Intersociety Conference on Thermal and Thermomechanical Phenomena in Electronic Systems, Orlando, FL, 2014.

J.R. Welling, C.B. Wooldridge, 1965. Free convection heat transfer coefficients from rectangular vertical fins, Trans. ASME J. Heat Transfer 87(3) (1965) 439-444.

S. Mostafa Ghiaasiaan, 2011. Convective Heat and Mass Transfer, Cambridge University Press. ISBN 978-1-107-00350-

A.A Mohammed, M.H. Hossam and EL-Khalil, 2018. The use of analytical hierarcial process to select the material for heatsink devices used in microelectronic. Proceedings of 136th The IRES International Conferences, Antalya, Turkey, 2018, pp 49-53.

G. Prashant Reddy and G. Navneet, 2010. Material selection for microelectronic heat sinks: An Application of the Ashby approach. Materials and Design. 31: 113-117.